Inelastic Scattering of 6- to 19-MeV Alpha Particles from Carbon*

G. E. MITCHELL,† E. B. CARTER,‡ AND R. H. DAVIS
Department of Physics, Florida State University, Tallahassee, Florida
(Received 7 October 1963)

The inelastic scattering of alpha particles from C^{12} was studied in detail. The 4.43-MeV gamma rays were observed from 6- to 17-MeV bombarding energy; the particles were observed from 10 to 19 MeV. Analysis of the gamma-ray data yielded the following specific conclusions: (1) Near 13.1-MeV excitation energy in O^{16} there is apparently a 2^+ level in addition to the well known 1^- level. (2) The 13.27-MeV level is 3^-, as previously reported. (3) The previously unassigned state at 13.88 MeV is 4^+. (4) A previously unreported level at 14.80 MeV has a low spin value. Numerous additional levels were found. The "two-channel" coupled equations approximation predicts many of the qualitative features of the particle angular distributions. Since the coupling is very strong, calculations for C^{12} illustrate well some of the features of this approximation.

I. INTRODUCTION

THE inelastic scattering of alpha particles from C^{12} is an interesting reaction from several viewpoints. One major interest lies in the compound states of O^{16}. Information concerning the levels of O^{16} is valuable because this nucleus is amenable to theoretical interpretation via shell, cluster, and alpha-particle models. The information gained by the study of this reaction supplements that obtained in the elastic scattering experiment on C^{12} (see previous paper[1]). More detailed discussion of the interpretation of the level structure of O^{16} is given in that paper.

Another major interest lies in the reaction mechanism for the inelastic process. The available alpha-particle energy for this experiment was nearly 20 MeV. Considerable experimental work on inelastic scattering has been performed at higher energies (see, for example, the review by Levinson[2]). On the contrary, inelastic alpha-particle scattering in the 10- to 20-MeV region is effectively unexplored. A survey at 18 MeV has been performed by the Purdue group.[3–5] Corelli's[5] data at 18 MeV for C^{12} suggest that the reaction mechanism is predominantly direct. Thus the transition region from mainly compound nuclear to mainly direct processes is available for study. In Sec. II, the $C^{12}(\alpha,\alpha_1\gamma_{4.43})C^{12}$ reaction is discussed. The apparatus, procedure, and errors are briefly examined, and the data presented. A similar procedure is followed for the inelastic reactions in which the particles were observed. Section III is devoted to an analysis of a portion of the gamma-ray data in terms of compound nuclear levels. Comparison is made with other relevant experimental work. In Sec. IV, an attempt is made to analyze the inelastic angular distributions (to the 2^+ state), using the coupled equations approach. This particular reaction shows in a rather striking fashion some of the features of coupled equations. Therefore, calculations on the $C^{12}(\alpha,\alpha_1)C^{12*}$ reaction are used to illustrate characteristics of the approximation. Typical results which predict most of the qualitative behavior of the inelastic angular distributions are presented. A brief summary is given in Sec. V.

II. APPARATUS, PROCEDURE, AND DATA

The $C^{12}(\alpha,\alpha_1\gamma_{4.43})C^{12}$ Reaction

The first few excited states in C^{12} are 2^+ at 4.43 MeV, 0^+ at 7.65, and 3^- at 9.6 MeV. The second excited state is above the threshold for breakup into $Be^8+\alpha$. The next several states above the 4.43-MeV state decay overwhelmingly by this particle channel. Therefore, the gamma-ray spectrum is very clean, even at relatively high alpha-particle bombarding energies.

For the gamma-ray experiment the targets were backed by a tantalum blank. Initially targets were prepared by a cracking process (heating the tantalum in a methyl iodide atmosphere). Targets prepared by this method contained an appreciable amount of oxygen. Targets were then prepared from a colloidal graphite dispersion. This reduced the oxygen content, as well as facilitated the preparation of large self-supporting foils.

At approximately 17 MeV, the $Ta(\alpha,n)$ reaction becomes prolific. The large yield of high-energy neutrons obscures the gamma-ray spectra rather badly. This is evidently a barrier penetration effect. A study by Carpenter[6] of this reaction from 15 to 19 MeV (using bismuth for collimation purposes, etc.) eliminated the need to extend this portion of the experiment beyond 17 MeV.

3-in.×3-in. NaI(Tl) crystals were used to detect the gamma rays, in conjunction with standard detection electronics. A typical pulse-height spectrum is shown in Fig. 1. For the excitation curve measurement, the

* Supported in part by the U. S. Air Force Office of Scientific Research. A significant portion of the analysis was performed while one of the authors (G.E.M.) held a visiting scientist appointment at the Oak Ridge National Laboratory.
† Present address: Columbia University, New York, New York.
‡ Present address: Rice University, Houston, Texas.
[1] E. B. Carter, G. E. Mitchell and R. H. Davis, Phys. Rev. **133**, B1421 (1964), preceding paper.
[2] C. A. Levinson in *Nuclear Spectroscopy*, edited by F. Ajzenberg-Selove (Academic Press Inc., New York, 1960).
[3] L. Seidlitz, E. Bleuler, and D. J. Tendam, Phys. Rev. **110**, 682 (1958).
[4] O. H. Gailar, E. Bleuler, and D. J. Tendam, Phys. Rev. **112**, 1989 (1958).
[5] J. C. Corelli, E. Bleuler, and D. J. Tendam, Phys. Rev. **116**, 1184 (1959).
[6] R. D. Carpenter, L. R. Mentillo, and E. Bleuler, Phys. Rev. **125**, 282 (1962).

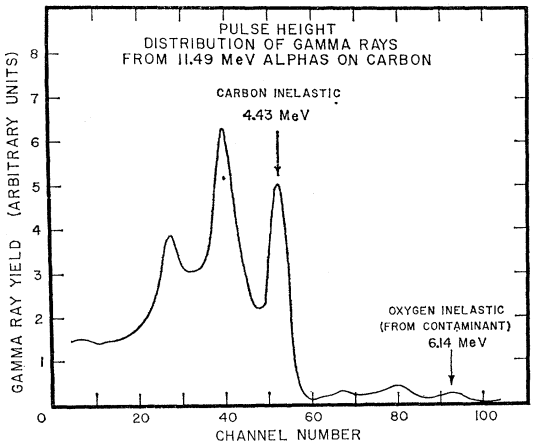

FIG. 1. Gamma-ray pulse-height spectrum.

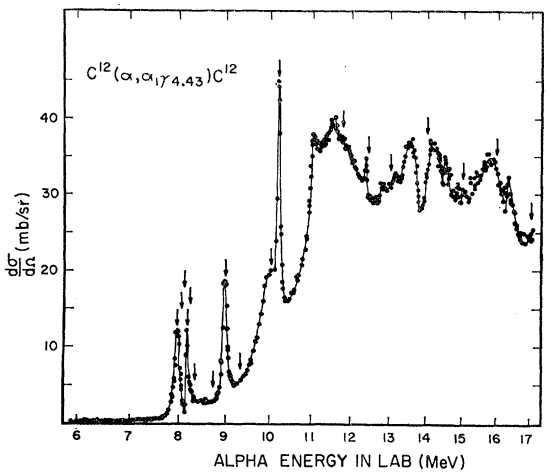

FIG. 2. Excitation curve for the $C^{12}(\alpha,\alpha_1\gamma_{4.43})C^{12}$ reaction. The arrows indicate energies at which angular distributions were measured.

crystal subtended an angle of $\pm 25°$. An estimate of the target thickness was obtained by using the known width of the 8.14-MeV level (13.25 MeV in O^{16}). Considering the observed width as due only to the intrinsic width (22 keV) and to the target, an approximate target thickness was determined. The targets for the gamma-ray excitation curve were about 50 keV thick to 8-MeV alpha particles.

The excitation curve is shown in Fig. 2. Below 11 MeV there are a number of well-resolved resonances; above 11 MeV there appear to be many (overlapping) levels. This curve was used as a guide in determining where to measure angular distributions. The arrows on the excitation curve indicate the energies at which

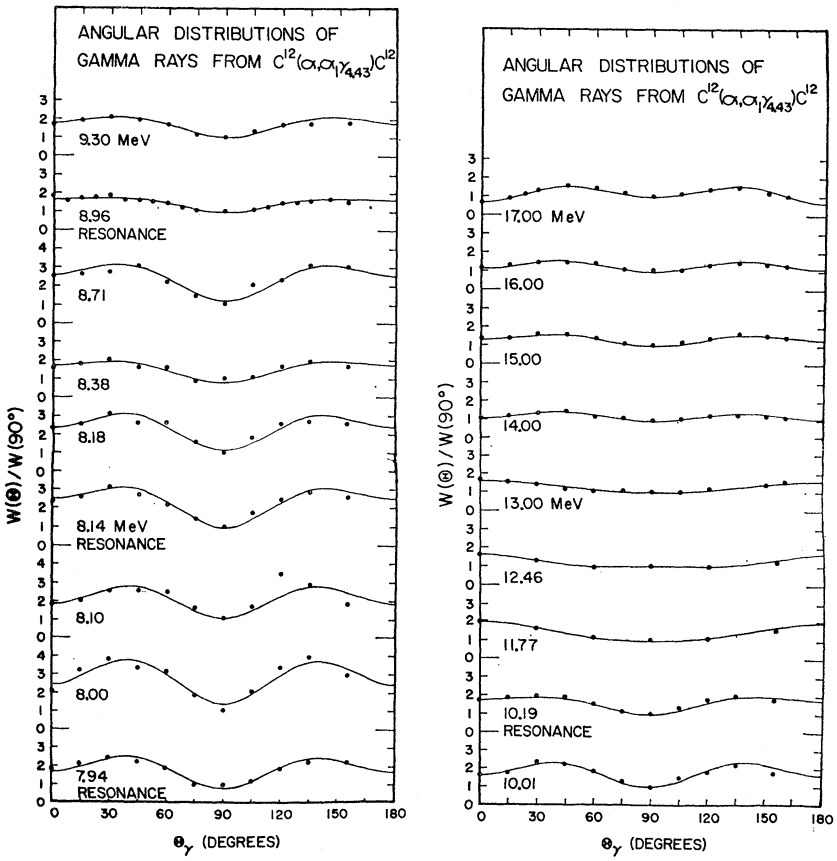

FIG. 3. Gamma-ray angular distributions—the solid curves are least-squares fit to even Legendre polynomials (to order 4).

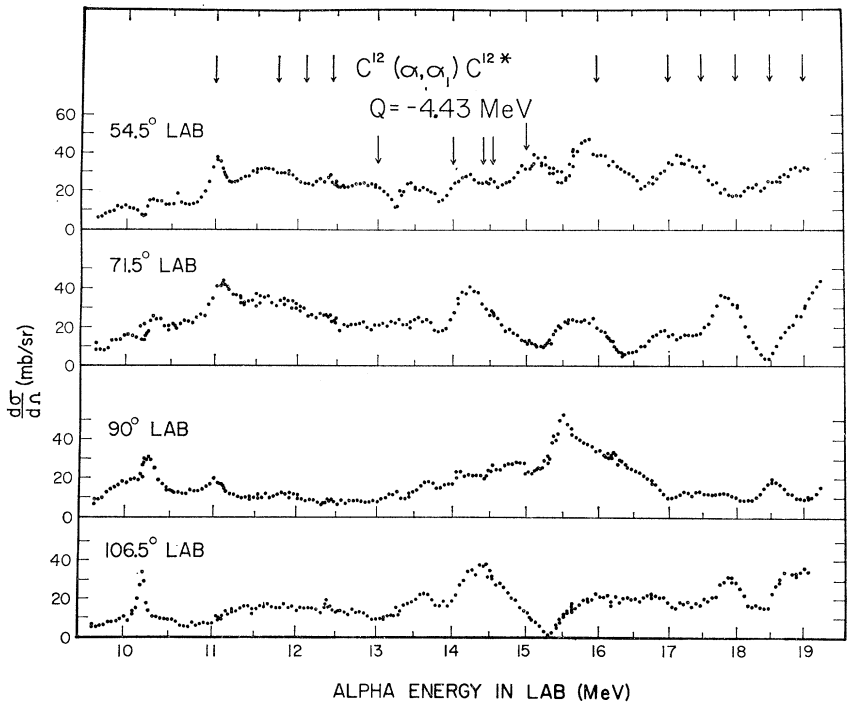

FIG. 4. Excitation curves for the first inelastic group. The arrows indicate the energies at which detailed angular distributions were measured.

angular distributions were measured. Relative errors for the excitation curve are listed in Table I.

TABLE I. Summary of relative errors.

Error (rms)	Gamma excitation curve	Gamma angular distribution	Particle excitation curves	Particle angular distribution
Integration	2%	2%	2%	2%
Counting statistics	3.5	5	3	4
Background subtraction	4	6	3	3
Carbon buildup	3		3	
Normalization	4			10
Angular errors		3		5
Gain changes	2			
Total geometric error			12	
Total	8%	9%	13%	14%

A small thin-walled brass chamber was used to measure the angular distributions. The target was mounted on a rotating frame, which was in electrical contact with the rest of the chamber, and the whole chamber used as a Faraday cup. One crystal was fixed at 90° to serve as a monitor. For most of the distributions, the rotating crystal was located at a distance of 12 in. The target thickness was again about 50 keV to 8-MeV alpha particles.

To facilitate comparison of shapes, each angular distribution was normalized to one at 90°. The data are presented in Fig. 3. The solid curves are least square fits to an expansion in even Legendre polynomials up to order four. The angular distributions in the lower energy region (of well-resolved resonances) fluctuate considerably with energy; those in the higher energy region are relatively constant. Note, however, the change in shape in the vicinity of 13 ot 14 MeV. The relative rms errors for the angular distributions are listed in Table I.

The $C^{12}(\alpha,\alpha_1)C^{12*}$ and $C^{12}(\alpha,\alpha_2)C^{12*}$ Reactions

The observation of the particles from the inelastic scattering reactions was performed in conjunction with the elastic scattering experiment. The apparatus and procedure are discussed in the previous paper. Here, only brief comments on these topics will be included.

Since the second inelastic group could be observed only at the higher energies and in a restricted range of angles, a detailed study was performed only on the first inelastic group. Excitation curves were measured at laboratory angles of 54.5° (79.6° c.m. at 10 MeV), 106.5° (136.3° c.m.), and 150° (165.1° c.m.) simultaneously, with a target which was approximately 63 keV thick to 10 MeV alpha particles. Excitation functions at 71.5° (101.0° c.m.), 90° (121.3° c.m.), and 125° (150.3° c.m.) were measured simultaneously with a target which was 175 keV thick to 10-MeV alpha particles. The center-of-mass angle is a function of the incident energy; the angular change is a decrease of approximately 5° from 10 to 19 MeV. Using the laboratory angle as a convenient label, the excitation curves are presented in Figs. 4 and 5. The excitation curves do show structure. Compared to the elastic-scattering data, however, the number and magnitude of the fluctuations are reduced. In Fig. 6, an excitation curve for

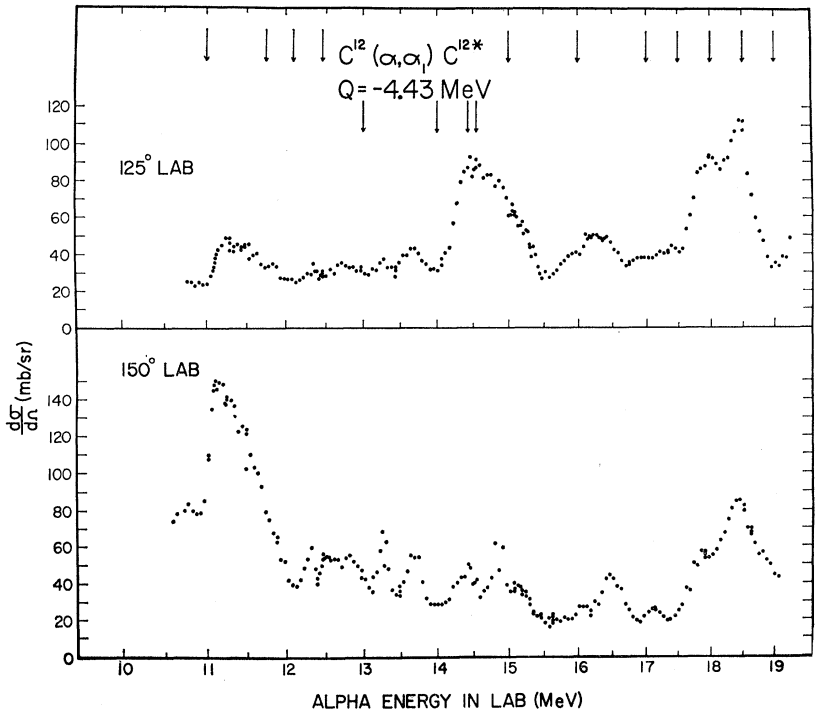

FIG. 5. Excitation curves for the first inelastic group at back angles. The arrows indicate the energies at which detailed angular distributions were measured.

the second inelastic group is shown. The broad anomaly around 17 MeV completely dominates this curve.

Fifteen angular distributions were measured, using targets which were about 100 keV thick to 10-MeV alpha particles. The inelastic angular distributions are presented in Fig. 7. A semilogarithmic scale is used for convenience. As compared to the elastic-scattering angular distributions, the inelastic distributions change relatively slowly with energy. The number of oscillations increases monotonically with energy. Moderate back angle peaking is often present. One angular distribution for the second inelastic group is shown in Fig. 8. Here the back angle peaking is very pronounced. The magnitude of the cross section for inelastic scattering to the second excited state is very small compared to scattering to the first excited state. Relative errors for both the excitation curves and angular distributions are included in Table I.

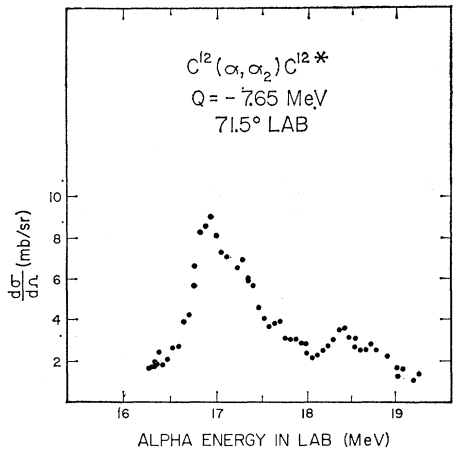

FIG. 6. An excitation curve for the second inelastic group.

Cross Sections and General Remarks

The procedure for determining the absolute cross section of the elastic scattering has been discussed in the previous paper. Using the cross sections for the elastic scattering, absolute cross sections for the inelastic scattering were evaluated. The details of normalizing excitation curves, angular distributions, and the gamma-ray excitation curve together are not important, except to note that the data are internally rather consistent. The absolute rms errors are estimated to be particle excitation curves—13%, particle angular distributions—12%, and gamma-ray excitation curve —14%. No attempt was made to place absolute cross sections on the gamma-ray angular distributions.

The cross sections may be compared with the results of Corelli.[5] The 18-MeV angular distributions obtained from the two experiments agree very well. The locations of the maxima and minima are the same; there is one discrepancy in magnitude of about 20% for the second maximum. However, the detailed shapes of the angular distributions are changing fairly rapidly with energy in this region, and the quoted energy resolution for the other experiment is about 1% (180 keV). Over all, the two experiments are in excellent agreement.

Some general conclusions may be drawn from the

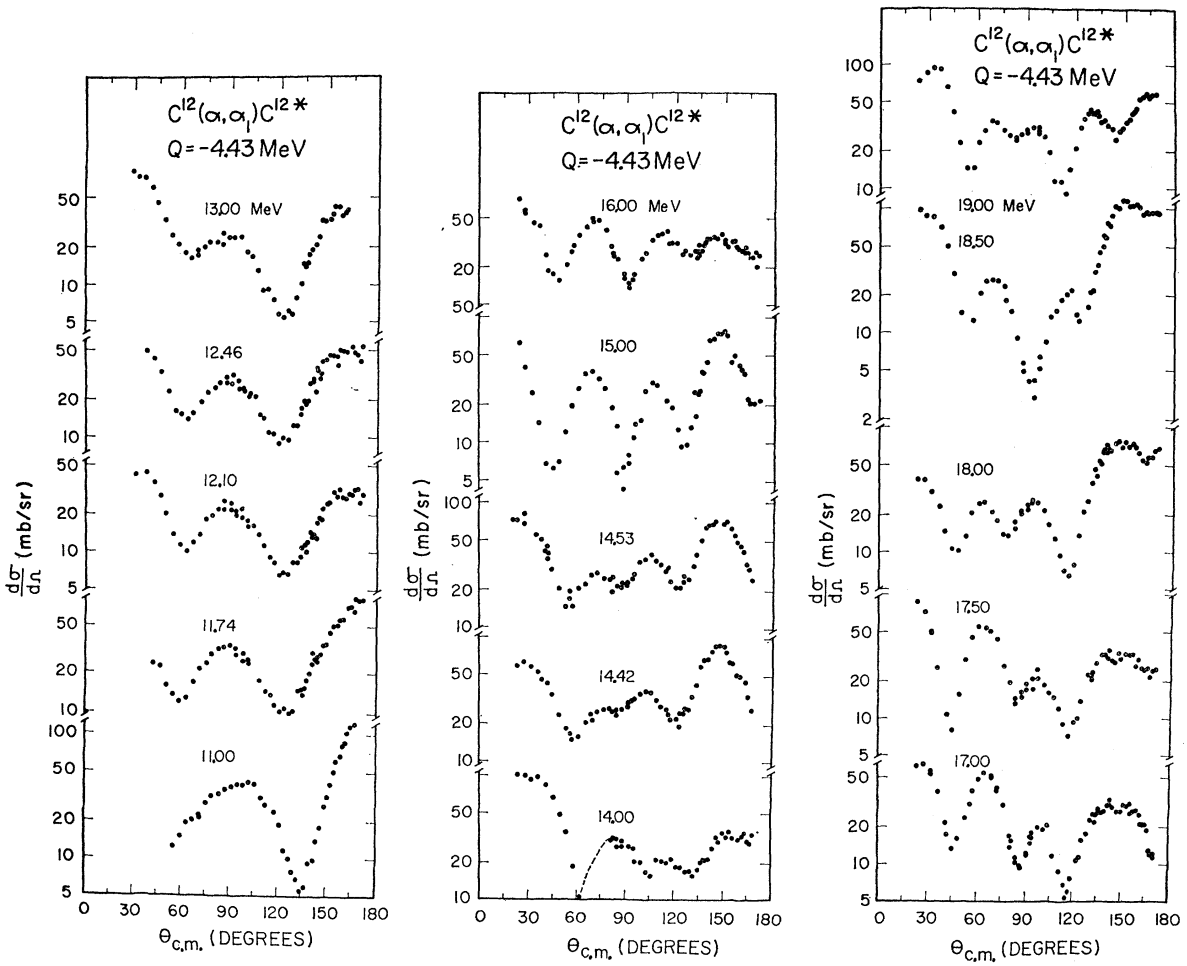

FIG. 7. Angular distributions for the first inelastic group.

experimental data. Below 11 MeV the gamma-ray excitation curve shows well-resolved resonances, and the angular distributions fluctuate with energy. The data clearly demand an interpretation in terms of compound nuclear levels. Above 11 MeV the gamma-ray and particle curves indicate the existence of many overlapping levels, although the structure is less pronounced than in the elastic-scattering data. The particle angular distributions change relatively slowly with energy; the change in the gamma-ray angular distributions is even slower. The magnitude of the inelastic cross section is very large. The data appear to suggest an interpretation in terms of a predominantly direct process. The analysis was approached from this general viewpoint.

III. ANALYSIS—LEVELS IN O^{16}

In the previous paper a detailed compilation is made of the levels in O^{16}. Here only the levels observed via the inelastic reaction are given. Table II summarizes the results. Several levels were not observed in the elastic scattering experiment, and these are denoted with an asterisk in Table II.

The gamma-ray angular distributions were fit with a Legendre polynomial expansion, using a least-squares program on an IBM 650 computer. The angular distribution has the form $W(\theta) \propto A_0b_0+A_2b_2P_2(\theta)+A_4b_4P_4(\theta)$ where the A's are the theoretical coefficients (for perfect geometry), and the b's are the attenuation coefficients which correct for the finite geometry.[7] The quantity A_ib_i was extracted by the least-squares program, and then divided by the appropriate attenuation coefficient. The results are tabulated in Table III. The resonances under detailed consideration occur in the region of 8- to 10-MeV bombarding energy. Since this corresponds to an excitation energy in O^{16} of about 13 to 15 MeV, a level may be labeled without ambiguity by either bombarding energy or excitation energy.

The formulation of Kraus[8] for the theoretical angular

[7] A. M. Feingold and S. Frankel, Phys. Rev. **97**, 1025 (1955).
[8] A. A. Kraus, Jr., J. P. Schiffer, F. W. Prosser, Jr., and L. C. Biedenharn, Phys. Rev. **104**, 1667 (1956).

TABLE II. Levels observed in the inelastic scattering reaction.

Gamma rays			Inelastic alphas		
E_{lab} (MeV)	E_{exc} (MeV)	J^π	E_{lab} (MeV)	E_{exc} (MeV)	Γ(MeV)
7.94	13.12	?			0.12
8.14	13.27	3^-			0.05
8.96	13.88	4^+			0.09
10.08	14.72				0.4
10.19	14.80	$0^+,1^-$	10.20	14.81	0.04
11.03	15.43		11.01	15.42	0.2
11.53	15.81		11.50	15.79	0.3–0.4
12.36	16.43		12.36	16.43	0.1
13.17	17.04		13.22	17.08	0.15
13.56	17.33		13.63*[a]	17.38	0.2
14.21	17.82		14.26*[a]	17.86	0.3
14.50	18.04		14.48	18.02	0.05
14.85	18.30		14.85	18.30	broad
15.07	18.46		15.13	18.51	broad
			15.51	18.79	broad
15.90	19.09		15.85*[a]	19.05	broad
			16.4*[a]	19.5	broad
			17.10	19.99	
			17.90	20.59	
			18.53	21.06	

[a] The asterisk denotes levels which were not also found in the elastic scattering experiment discussed in the previous paper.

distributions was followed. In this reaction, only natural parity compound nuclear states may be formed. Since the entrance and exit channel spins are unique (0 and 2, respectively), the expected angular distribution for a single level is rather simple. The only complication is the incoherent addition of the contributions from the various possible exit orbital angular momenta. Since in this energy region the emitted alpha particles have an energy which is relatively low compared to the combined Coulomb and angular momentum barrier, only the lowest possible exit angular momentum contributes appreciably. This will be made quantitative in connection with each resonance. The theoretical angular distributions corresponding to various J^π and exit orbital angular momenta are given in Table IV.

TABLE III. Coefficients extracted from a least squares fit to the gamma-ray angular distributions. Finite geometry corrections are included.

E(MeV)	A_2/A_0	A_4/A_0
7.94	0.620±0.070	−0.527±0.084
8.00	0.489 0.058	−0.605 0.072
8.10	0.463 0.076	−0.648 0.102
8.14	0.684 0.052	−0.541 0.063
8.18	0.572 0.096	−0.522 0.116
8.38	0.546 0.117	−0.375 0.153
8.71	0.688 0.070	−0.574 0.090
8.95	0.405 0.033	−0.218 0.040
9.30	0.483 0.033	−0.379 0.040
10.01	0.461 0.045	−0.542 0.056
10.19	0.482 0.015	−0.332 0.019
11.77	0.497 0.027	0.132 0.033
12.46	0.310 0.028	0.221 0.035
13.00	0.337 0.028	0.056 0.044
14.00	0.168 0.042	−0.252 0.053
15.00	0.307 0.020	−0.316 0.025
16.00	0.210 0.020	−0.352 0.025
17.00	0.059 0.015	−0.526 0.020

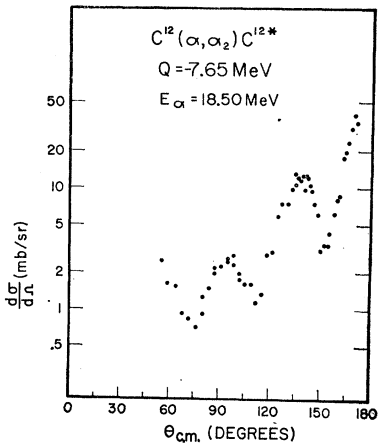

FIG. 8. Angular distribution at 18.50 MeV for the second inelastic group.

Information on the natural parity levels of O^{16} in this region of excitation energy has been obtained primarily from studies of N^{15} plus proton reactions.[9–13] The combined relevant results may be briefly summarized: 13.0-MeV excitation energy (1^-), 13.25-MeV (3^-), 13.89-MeV (possible natural parity level, appears very weakly in the p,α_0 reaction).

TABLE IV. Theoretical coefficients for gamma-ray angular distributions.

J^π,l'	A_2/A_0	A_4/A_0
0^+, 2	...	...
1^-, 1	0.500	...
1^-, 3	0.143	...
2^+, 0	0.714	−1.714
2^+, 2	−0.153	−0.490
2^+, 4	0.204	−0.014
3^-, 1	0.571	−0.571
3^-, 3	−0.263	−0.571
3^-, 5	0.238	−0.026
4^+, 2	0.510	−0.367
4^+, 4	−0.301	−0.601
4^+, 6	0.260	−0.036

Spicer[14,15] studied the $O^{16}(\gamma,p)N^{15}$ reaction and found a strong resonance at about 14.7 MeV. Subsequent to the present gamma-ray experiment, Larson[16] examined the $C^{12}(\alpha,\alpha_1\gamma_{4.43})C^{12}$ reaction in connection with a capture gamma experiment on C^{12}. The location of the levels observed by Larson agree very well with the results of the present experiment.

The experiment most relevant to the present work

[9] S. Bashkin and R. R. Carlson, Phys. Rev. **106**, 261 (1957).
[10] F. B. Hagedorn, Phys. Rev. **108**, 735 (1957).
[11] F. B. Hagedorn and J. B. Marion, Phys. Rev. **108**, 1015 (1957).
[12] S. Bashkin, R. R. Carlson, and R. A. Douglas, Phys. Rev. **114**, 1543 (1959).
[13] R. Weinberg, H. Dieselman, C. Nissim-Sabat, and L. J. Lidofsky, Bull. Am. Phys. Soc. **6**, 27 (1961).
[14] B. M. Spicer, Phys. Rev. **99**, 33 (1955).
[15] B. M. Spicer (private communication).
[16] J. D. Larson and R. H. Spear, Bull. Am. Phys. Soc. **6**, 505 (1961).

was performed by Ferguson and McCallum.[17,18] The elastic and inelastic scattering of alpha particles from C^{12} was observed from 6 to 11 MeV. Their results may be summarized (for the present purposes): levels at 13.10-MeV excitation energy (1^- and 2^+), 13.27 MeV (3^-), 13.90 MeV (4^+), 14.7 MeV (natural parity level), 14.83 MeV (0^+).

The general agreement with other experimental work is excellent. More natural parity states are seen in the C^{12} plus alpha reaction than in the N^{15} plus proton reaction. These additional levels evidently have rather small proton widths.

13.10-MeV Region

The experimental results fit very well an assumed 3^- state, with $l'=1$ ($l'=1$ is more than 20 times as probable as $l'=3$ at this energy). All previous results identified this level as 1^-. Furthermore, this state is taken to be $T=1$—the analog of the low-lying 1^- state in N^{16}. There is no other known 1^- level in this region of O^{16}.

A 1^- state could interfere with the nearby 3^- level (only states of the same parity may interfere in this reaction, see Ref. 7). However, the interference would have to be very strong in order to explain the shift of the experimental angular distribution. The 3^- level is not changed from its expected shape. Ferguson and McCallum[18] assumed two states, 1^- and 2^+, in order to explain their data. They suggest that a linear combination of effects from the two levels (which do *not* coherently interfere) could explain the results of the present experiment. Indeed, there is a very simple combination which will reproduce the experimental results: $\frac{2}{3}W(1^-)+\frac{1}{3}W(2^+)=W(3^-)$. The lowest possible l' values are assumed. However, it is impossible to verify this hypothesis from the present data. If there are two levels, 1^- and 2^+, then the present results simply determine the ratio of the two S matrix elements involved. That is, $|S(1^-)/S(2^+)|^2=k$, where the constant depends upon the known statistical weights, etc., and upon the empirically determined ratio of the relative importance of the two angular distributions (by hypothesis, about 2).

13.27-MeV Level

The coefficients extracted from the experimental data agree best with $J^\pi=3^-$ and $l'=1$. At this energy, $l'=1$ predominates over $l'=3$ by more than 10. The assignment is 3^-, which agrees with all previous results.

13.88-MeV Level

Since this level is seen here very clearly, it must have a very small partial width for proton emission (in order to explain its near absence in N^{15} plus proton reactions). The experimental results are closest to the predictions for $J^\pi=4^+$ and $l'=2$. For this energy, $l'=2$ predominates over $l'=4$ by a factor of more than 20. The assignment is 4^+, which agrees with Ferguson's independent assignment.

14.7- to 14.8-MeV Region

In the region around 10.1- to 10.2-MeV bombarding energy, there are at least two levels. There is a narrow resonance at 10.19 MeV (14.80 in O^{16}) and a broader resonance at about 10.08 MeV (14.72 in O^{16}). The gamma-ray angular distributions are not sufficient to extract much information about these two levels. The emitted alpha particle has an energy near the top of the barrier (therefore more than one l' value contributes appreciably), there are two levels, and both of these levels are riding on a rapidly increasing background. As a first approximation, the angular distribution on the peak of the broad level was subtracted from a distribution on the peak of the narrow level. The difference is considered as approximately due to the 10.19-MeV resonance. The result is nearly isotropic, and thus most consistent with a low spin assignment. Ferguson's assignment for this level is 0^+. The broad level is not yet assigned.

The 1^- level at 13.10-MeV excitation energy and the 3^- level at 13.25 MeV are considered the analogs of the second and third excited states of N^{16} (the order is inverted in the two nuclei). Since these $T=1$ states are seen very clearly in this reaction which involves only $T=0$ particles, there must be appreciable isospin mixing at this excitation energy in O^{16}.

IV. ANALYSIS—DIRECT REACTION

The particle angular distributions change relatively slowly with energy. The over-all trend may be observed by plotting the locations of the maxima and minima as a function of energy. This is done in Fig. 9 (the higher energy data is from Mikumo[19]).

There have been numerous discussions of direct inelastic scattering recently.[2,20–24] The most widely successful approach to direct reactions has been the distorted-wave Born approximation (DWBA). The transition amplitude is assumed to have the form $\langle\chi_f(r)\psi_f(\zeta)|V(r,\zeta)|\chi_i(r)\psi_i(\zeta)\rangle$, where ψ_i and ψ_f are the nuclear wave functions, χ_i and χ_f are the distorted wave functions (of relative motion), and V is the "residual" interaction which causes the transition. The distortion is usually considered as caused by an optical potential.

[17] A. J. Ferguson and G. J. McCallum, Bull. Am. Phys. Soc. **6**, 235 (1961).
[18] A. J. Ferguson (private communication).
[19] T. Mikumo, J. Phys. Soc. Japan **16**, 1066 (1961).
[20] E. Rost and N. Austern, Phys. Rev. **120**, 1375 (1960).
[21] R. H. Lemmer, A. DeShalit, and N. S. Wall, Phys. Rev. **124**, 1155 (1961).
[22] W. Tobocman, *Theory of Direct Nuclear Reactions* (Oxford University Press, London, 1961).
[23] R. H. Bassel, G. R. Satchler, R. M. Drisko, and E. Rost, Phys. Rev. **128**, 2693 (1962).
[24] E. Rost, Phys. Rev. **128**, 2708 (1962).

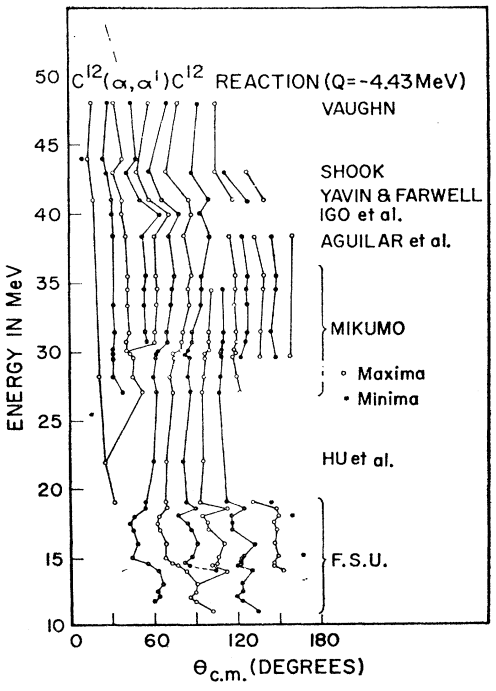

FIG. 9. Angular positions of maxima and minima as a function of energy. The data above 20 MeV is taken from Ref. 19.

The optical parameters are determined by fitting the elastic-scattering data (in the entrance and exit channels), and then used in the DWBA calculation.

The residual interaction is assumed to be small. However, the cross section for inelastic scattering from C^{12} is very large. Some typical integrated cross sections are 330 mb (at 13 MeV), 430 mb (14 MeV), 266 mb (15 MeV), 420 mb (16 MeV), and 370 mb (17 MeV). It seems doubtful that any Born approximation is valid for this reaction.

Coupled-Equations Analysis

An alternative approach is offered by coupled equations analysis.[25] Buck[26–28] has developed this approach and coded the problem for an IBM 7090 computer. This approximation may be described as a generalized optical model in which an excited state is strongly coupled to the nuclear ground state. In particular, a state of quadrupole collective motion is considered. The resulting set of coupled equations are solved numerically. The matrix elements of the scalar part of the interaction are taken to be the usual optical model potentials.

The quadrupole portion is that which causes the direct transition. Explicit values for the strengths $V_{II'}$ of these matrix elements are found through the use of a definite nuclear model. For a simple rotational model, $V_{II'} \propto \beta V_0 R_0/a$, where β is the usual deformation parameter, V_0 is taken to be the depth of the real optical potential, and R_0 and a are the radius and diffuseness associated with V_0. The matrix elements V_{02} and V_{22} differ by a simple numerical factor. In a simple vibrational model, for an equivalent deformation parameter, V_{02} has the same form. Since a single creation or destruction operator can only link states (N is the phonon number) $|N>$ to $|N\pm1>$, V_{22} must be zero. The value for V_{22} selects the model; the sign of β determines the kind of deformation (in the vibrational model, the sign of β will correspond only to a phase change). DWBA has no term corresponding to V_{22}, and thus makes no distinction between the two models.

The optical potentials are assumed to be the same in the entrance and exit channels. The optical model parameters can be conveniently combined into groups of three—a potential (MeV), a radius (F), and a diffuseness (F). There is a real potential with a Saxon shape (V_s,R_{sp},A_s), an imaginary potential with a Saxon shape (W_i,R_{ip},A_i), and an imaginary potential with a form factor proportional to the derivative of the Saxon shape (W_d,R_{dp},A_d). Radii are defined according to the convention $R=R_0A^{1/3}$. The Coulomb scattering is taken to be that from a uniformly charged sphere of radius R_{sp}. The shape of the residual interaction is taken to be the derivative with respect to (r/A) of a Saxon potential: Different parameters A_{in} and A_{ex} are assumed for r less than or greater than R_{ap}, the radius for the residual interaction.

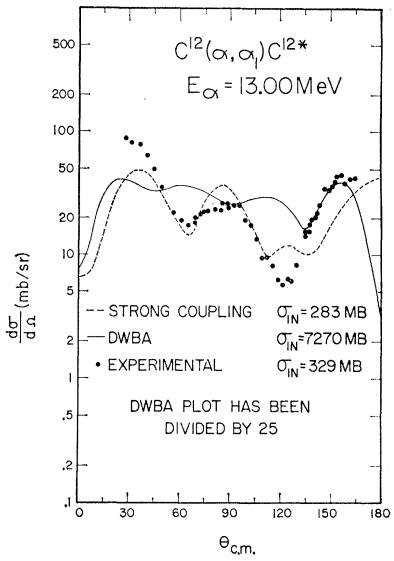

FIG. 10. A comparison between the strong coupling approximation and a (simulated) DWBA calculation. The parameters are discussed in the text. For the strong coupling calculation the parameters were: $E=13.00$, $Q=-4.43$, $V_s=125$, $W_i=1$, $W_d=0$, all radius constants $(R/A^{1/3})=1.87$, all diffusenesses $=0.5$, $\beta=0.45$, vibrational model. The parameters were the same for the simulated DWBA calculation, except $\beta=0.01$. The latter results were scaled by $(0.45/0.01)^2$.

[25] D. M. Chase, L. Wilets, and A. R. Edmonds, Phys. Rev. **110**, 1080 (1958).
[26] B. Buck, Phys. Rev. **127**, 940 (1962).
[27] B. Buck, Phys. Rev. **130**, 712 (1963).
[28] B. Buck (private communication).

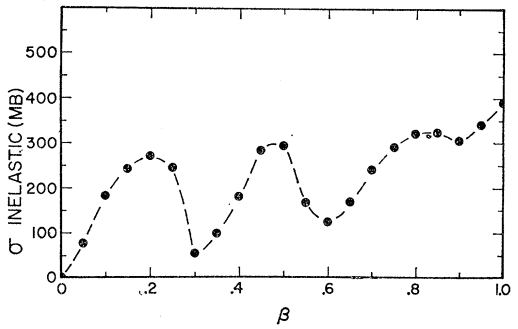

FIG. 11. The inelastic cross section as a function of β. The parameters were: $E=13.00$, $Q=-4.43$, $V_s=125$, $W_d=0$, all radius constants $=1.87$, all diffusenesses $=0.5$, β variable, vibrational model.

In the previous paper it was shown that to even begin to fit the elastic scattering data with an optical model, the real potential must be very large, and the imaginary potential (s) very small (about 100 MeV and a few MeV, respectively). These approximate values were used as a first approximation for coupled equations calculations.

In addition to the features of the elastic and inelastic scattering, the reaction cross section must be correctly predicted. The "residual" reaction cross section (excluding inelastic scattering to the first excited state) is not known. However, the magnitude of this cross section is probably at most a few hundred mb. Sets of parameters which yielded more than this value were rejected.

To anticipate, the results of the coupled equations analysis display the qualitative features of the inelastic-scattering data, but the quantitative agreement is not good. However, it is interesting to examine to what extent this approximation can describe the experimental results.

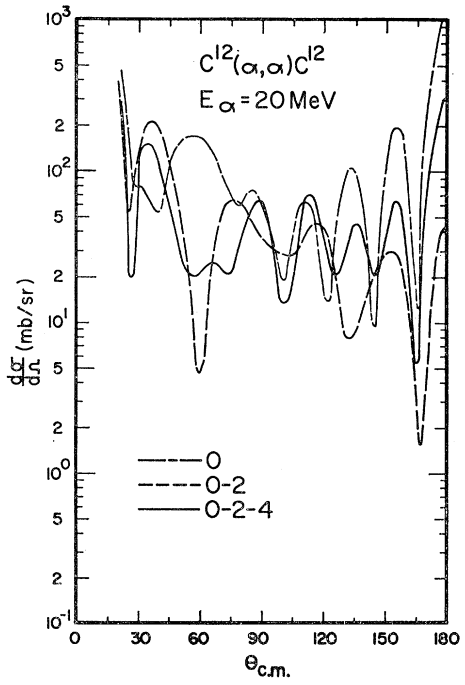

FIG. 12. The effect on elastic scattering of coupling additional states. For elastic scattering only, the parameters were: $E=20.00$, $V_s=130$, $W_s=0$, $W_d=0.64$, all radius constants $=1.87$ (except the residual interaction radius constant $=1.93$), all diffusenesses $=0.5$ (except $A_{ex}=0.4$). For the two-channel case, a 2^+ rotational state at 4.43 MeV is included. For the three-channel case, a 4^+ rotational state is included at 13.00 MeV. The deformation parameter is 0.55. Other parameters remain the same for different cases.

Comparison of DWBA and Coupled-Equations Analysis

It is also of interest to compare the results of a DWBA calculation with the data. This was regarded as a special case in coupled equations analysis since the strong coupling approximation formally reduces to the DWBA for very small β (weak coupling). A set of parameters which gave qualitatively correct results at 13 MeV was used, and the inelastic cross section calculated with $\beta=0.01$. In DWBA, β is just a scale factor. Therefore, a simulated DWBA calculation was achieved by scaling these results by $(0.45/0.01)^2$. The strong coupling result was σ inelastic $=283$ mb (experimental value $330\pm20\%$ mb). The simulated DWBA value is σ inelastic $=7270$ mb, and the computed angular distribution is shown in Fig. 10. The same optical-model parameters were used in both the coupled equations and DWBA calculations. A self-consistent DWBA analysis[29] with a different set of optical-model parameters should yield results in better agreement with the data.

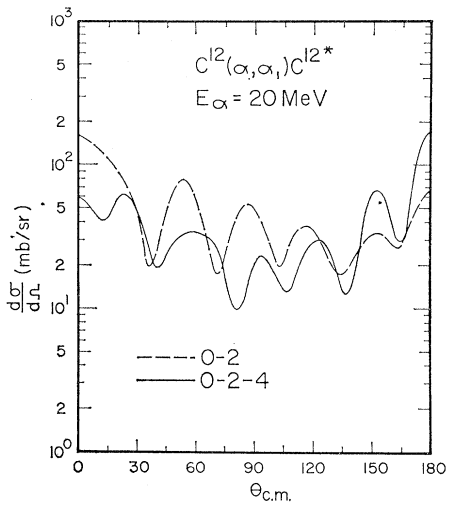

FIG. 13. Effect on the inelastic scattering of coupling additional states. The parameters are the same as in Fig. 12.

[29] F. Perey and G. R. Satchler, Phys. Letters 5, 212 (1963).

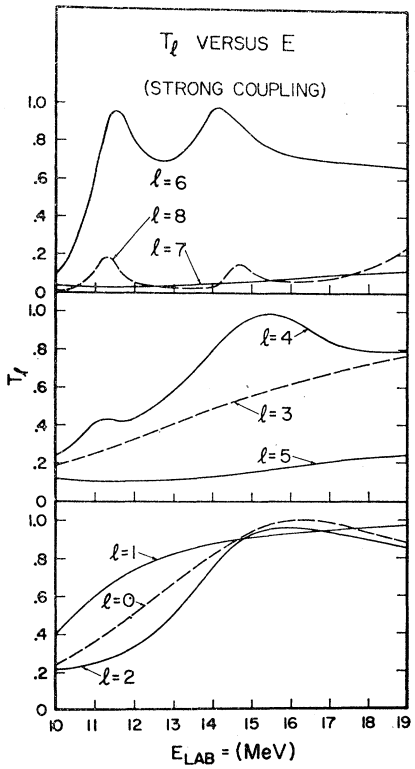

FIG. 14. Plot of transmission coefficients versus energy. The parameters were: $V_s=130.5$, $W=0$, $W_d=0.65$, all radius constants $=1.87$ (except the residual interaction radius constant $=1.93$), all diffusenesses $=0.5$ (except $A_{ex}=0.4$), $\beta=0.595$, vibrational model.

Influence of a Third Level

The dependence of σ inelastic on β is different in the two approximations. In DWBA, the cross section is proportional to β^2. Results with coupled equations[27] show a saturating effect in which the inelastic cross section becomes more nearly proportional to β, rather than β^2. As shown in Fig. 11, here the cross section actually oscillates with β. The coupling is clearly very strong. The large discrepancy between coupled equations (in the region of deformation near 0.5) and DWBA is obvious. On the other hand, the two-channel approximation used here may also be in difficulty. In the "two-channel" coupled equations approximation, changes in the inelastic cross section have a rather large "feedback" effect on the elastic scattering. This may be realistic. However, if there are other states strongly coupled, then the effect on the elastic channel might be quite different.

To examine this question, a set of calculations were performed to study the effect of coupling additional states. A 4^+ rotational state at 13.00 MeV was *assumed*.[30] The procedure was as follows: First, only the elastic scattering was considered (no coupling), then the 2^+ state at 4.43 MeV was included (0^+-2^+), then the 4^+ state at 13.00 MeV was also included ($0^+-2^+-4^+$). Since the $0-2-4$ code had no provisions for including the effects of states below threshold ($\sim$17.3 MeV for 4^+ state), the bombarding energy was assumed to be 20 MeV.

The results for the elastic and inelastic scattering are shown in Figs. 12 and 13. The introduction of the 2^+ state has a large effect on the elastic scattering, as does the addition of the 4^+ state. The effect on the inelastic scattering is somewhat less pronounced. Qualitatively similar results were obtained when a 4^+ vibrational state was assumed at 9 MeV. In the rotational example, the calculated inelastic cross section to the 2^+ state was about 300 mb, while the cross section to the 4^+ state was approximately 10 mb. Although the cross section to the 4^+ state is almost negligible, this state has a large effect on the elastic scattering. Thus, the magnitude of the cross section may be very misleading as an estimate of the influence of a reaction channel. In particular, some states in C^{12} which are observed weakly or not at all in this experiment may be essential to a fitting of the elastic-scattering data (with this analysis). These results also show (at least for direct inelastic scattering) that a small cross section is *not* a sufficient condition for the validity of DWBA. At least part of the difficulty is presumably kinematic. Well above threshold the magnitude of the cross section should be a much better gauge.

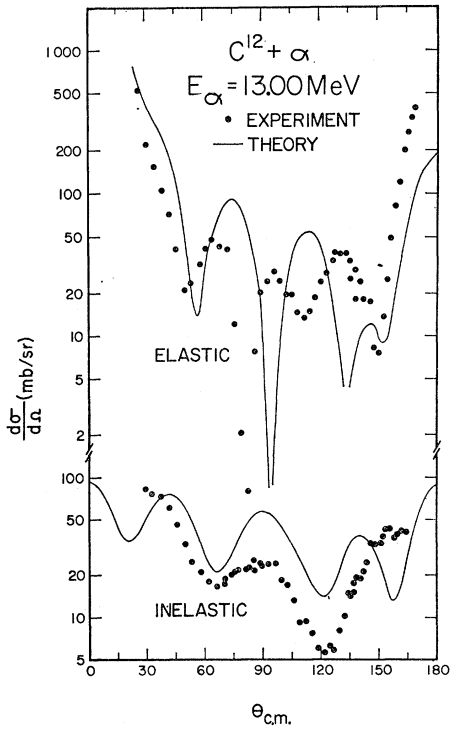

FIG. 15. Comparison between theory and experiment at 13.00 MeV. The parameters were $V_s=130$, $W_i=0$, $W_d=0.25$, all radius constants $=1.87$, all diffusenesses $=0.5$, $\beta=0.45$, vibrational model.

[30] A 4^+ state at 14 MeV has been observed by K. H. Wong, S. D. Baker, and J. A. McIntyre, Phys. Rev. **127**, 187 (1962); and by G. T. Garvey, A. M. Smith, and J. C. Hiebert, Phys. Rev. **130**, 2397 (1963).

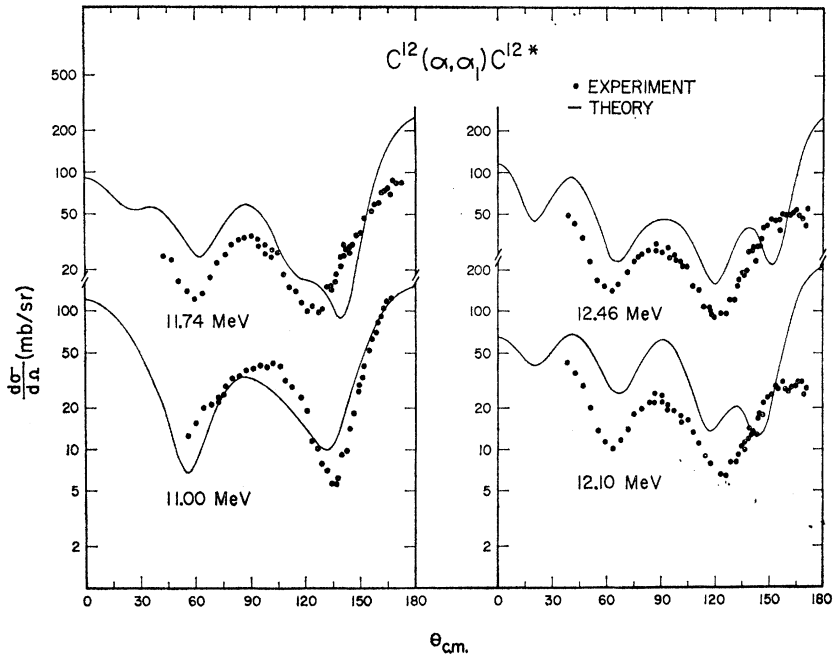

FIG. 16. Comparison between theory and experiment at several energies. The parameters are the same as in Fig. 15.

Coupling Resonances

Another interesting result of the coupled equations formulation is the appearance of "coupling" resonances in the theoretical excitation curves. Typical results are shown in Fig. 14, where the transmission coefficients are plotted versus energy. These transmission coefficients are somewhat different from usual, in that both elastic and first inelastic channels are treated as "scattering" (the analogue of elastic scattering in the usual case). Several of the resonances are narrow, and cannot be predicted by an optical model. Detailed optical-model calculations bear this out. Buck[28] observed these resonances, as did Okai and Tamura.[31] Since the latter observe these effects in a simplified calculation using square wells for the optical potentials and a delta function for the direct interaction, these resonances are evidently a general property of the coupling. No attempt has yet been made to correlate these "coupling" resonances with the present data. There are many resonances observed experimentally which have appropriate widths and it is possible that some or many of these are indeed due to the coupling.

Comparison with Experiment

At the time these calculations were performed, it was not known where the appropriate 4^+ state in C^{12} was located. The existing codes were limited to 0^+, 2^+, 4^+ states, which precluded the possibility of including other known states in C^{12}. Therefore, attempts were made to fit the data using the 0–2 code.

Exhaustive efforts were not made to fit the data. Some typical results are shown in Figs. 15 and 16. The elastic-scattering fit is very poor. However, the inelastic fits are qualitatively correct in shape and magnitude. The energy variation is not inconsistent with the data. Typical residual reaction cross sections are about 150 mb. As expected when the two processes are so closely interwoven, improving fits on the elastic usually worsens the fit to the inelastic, and vice versa. One serious difficulty is the effect of other strongly coupled states which are not included in the calculation.

In the preceding paper it was shown that the elastic scattering angular distributions could be fit reasonably well by including the effects of individual resonances. These resonances are probably the prime source of difficulty in fitting the elastic scattering with the "two-channel" coupled equations approximation. Although the direct mechanism appears to predominate for the inelastic scattering, the compound nuclear effects appear to be strong enough to preclude successful quantitative fitting of both the elastic and inelastic scattering with the present approximation.

V. SUMMARY

This experiment was motivated by a dual interest—in the energy levels of O^{16}, and in the reaction mechanism for the inelastic process. Below 11-MeV bombarding energy compound nuclear processes predominate. Above 11 MeV the mechanism is predominantly direct, with appreciable amounts of compound nuclear effect also contributing.

Analysis of the gamma-ray angular distributions yielded the following results of interest: (1) Near 13.1-MeV excitation energy in O^{16}, there is apparently a

[31] S. Okai and T. Tamura, Nucl. Phys. **31**, 195 (1962).

previously unreported 2^+ level in addition to the well known 1^- level. (2) The 13.88-MeV level has a spin and parity of 4^+. (3) The previously unreported level at 14.80 MeV is either 0^+ or 1^-. The simultaneous experiment by Ferguson[17,18] yielded nearly identical results.

Several general features of the coupled-equations approach are well illustrated by the $C^{12}(\alpha,\alpha_1)C^{12*}$ reaction. DWBA overestimates the cross section by more than an order of magnitude at these energies (this is no longer true at higher energies). The coupling of additional states has a pronounced effect on the elastic scattering, even when the inelastic cross section is small. Many of the qualitative features of the experimental data (shape, magnitude, energy dependence) are correctly reproduced. Explicit consideration of only two channels, and compound nuclear effects preclude detailed quantitative agreement. Compared to DWBA, however, the "two-channel" coupled-equations approximation is fairly successful.

ACKNOWLEDGMENTS

The authors would like to thank Dr. W. E. Hunt, Dr. M. K. Mehta, J. D. Marshall, and J. B. Seaborn for assistance in performing the experiment; S. Brudno for aid in the computing performed at Florida State University; and Dr. S. Edwards, Dr. N. R. Fletcher, Dr. J. D. Fox and Dr. J. W. Nelson for valuable discussions.

One of us (G.E.M.) would like to thank the Oak Ridge Institute of Nuclear Studies for financial assistance; Dr. B. Buck for the use of his computer programs; D. E. Arnurius for assistance with the computing performed at Oak Ridge; and Dr. Buck and Dr. G. R. Satchler for numerous invaluable discussions.

PHYSICAL REVIEW VOLUME 133, NUMBER 6B 23 MARCH 1964

Double Stripping: (He^3,n) Reaction*

ERNEST M. HENLEY AND DAVID U. L. YU
University of Washington, Seattle, Washington
(Received 6 November 1963)

The two-nucleon stripping reaction is examined in detail, with particular reference to the (He^3,n) reaction. Three models are studied and compared: (1) the plane-wave Born approximation, (2) the distorted-wave Born approximation, and (3) a simple diffraction model. Zero-range approximations are not assumed *a priori*. For (1) and (2), the wave functions of the two captured nucleons are taken to be eigenstates of an infinite harmonic oscillator, the strength of which is adjusted to reproduce single-particle eigenfunctions of a finite Saxon well in regions close to the nuclear surface. The first model is primarily employed to show that the modulation of the angular distribution due to the structure of He^3 is also sensitive to the form and range of the stripping interaction. Model (2) is used to calculate absolute differential cross sections to various final states, in particular for C^{12}, O^{16}, Ni, and Sn targets with 20-MeV incident He^3 ions. Comparison with experimental data is made where available and agreement is found. To further such comparisons we also compute summed cross sections to several low-lying states of the final nucleus. Spectroscopic weights are obtained for pure and mixed configurations of single-particle wave functions. Model (3) provides insight into the dominant features of the experimental and calculated [model (2)] differential cross sections. These are: (a) a strong forward peaking of the distribution especially for spin 0 to 0 transitions, but also for summed cross sections, (b) an angular distribution for such sums that is roughly independent of the atomic weight of the target nucleus, and (c) an enhancement of cross sections to higher spin states ($\approx$3 or 4) of final nuclei. These features are not reproduced with model (1).

I. INTRODUCTION

THE use of deuteron projectiles for studying nuclear spectroscopy is well known. Recently, attention has focused on the double stripping reaction for the same purpose. In fact, it has been pointed out by Yoshida[1] that double stripping may be particularly suited to the study of collective (vibrational) levels.

Although considerable experimental investigation of the two-nucleon stripping reaction has already taken place, all theoretical analyses to date use the plane-wave Born approximation to describe the process. This, even though not valid, is of some use for obtaining level spin assignments from angular distribution in deuteron stripping. However, it is not known whether the same information can be extracted from the application of the Born approximation to two-nucleon stripping processes.

In this paper we shall examine the two-nucleon stripping reaction in detail. In Sec. II we first develop a general formulation of the double-stripping reaction, which we specialize to the (He^3,n) process as a particular example. We do not make any zero-range approximations. We use a Gaussian for the internal wave function of He^3 as well as for the stripping interaction. For the

* Supported in part by the U. S. Atomic Energy Commission under Contract A. T. (45-1)1388, Program B.
[1] S. Yoshida, Nucl. Phys. **33**, 685 (1962).